The Shape of Ibuprofen in the Gas Phase - Supplementary Material

Thomas Betz, Sabrina Zinn, and Melanie Schnell

Max Planck Institute for the Structure and Dynamics of Matter, Luruper Chaussee 149, D-22761 Hamburg

The Hamburg Centre for Ultrafast Imaging, Luruper Chaussee 149, D-22761 Hamburg

Center for Free-Electron Laser Science, Notkestrasse 85, D-22607 Hamburg

Contents

1 Ibuprofen Monomer

1.1 Structure Calculations

For characterizing the conformational landscape of ibuprofen, ab initio calculations were carried out. In the following, we summarize the results of these calculations. To get various starting points for the geometry optimization of ibuprofen, rotations around single bonds in the molecule were done. From these calculations, we obtained twelve low energy conformers of ibuprofen. The results using the M06-2X level of theory can be found in Table 1 of this Supplementary Material.

For comparison reasons, the conformers of ibuprofen are labeled according to the following code, which reflects the orientations of the functional groups in the molecule:

OH/O

- either the carboxy-group oxygen (O) or the hydroxy-group oxygen (OH) points towards the α-methyl top of the propanoic acid group.

C/T

- indicates the cis (C) or trans (T) orientation of the isobutyl group and the carboxy group with respect to the aromatic ring plane.

C/B

- This label describes the orientations of the isobutyl group. The label B (branched) indicates that both methyl tops of the isobutyl group are pointing away from the phenyl ring. This leads to a branched structure that is symmetric with respect to the phenyl ring. The label C (chain) indicates an elongated chain structure, where one methyl top of the isobutyl group is pointing away from the phenyl ring.

c/t

- labels the two possible orientations in the chain configuration, where a cis (c) or a trans (t) configuration of the methyl top in the isobutyl group with respect to the carboxy group of the propanoic acid group can exist. This difference does not exist for the B configuration because of its symmetry towards the phenyl ring.

Two examples for the labeling system are depicted in Figure 1.

The four lowest-energy conformers are experimentally observed. The next group of conformers is 1.5 kJ/mol higher in energy and is not sufficiently populated anymore in our molecular jet (see Table 1).

Calculations using the B3LYP functional show larger deviations of the theoretical values from the experimental ones than obtained for the M06-2X functional. Especially the absolute values of the rotational constants are not reproduced accurately, while the difference between B and C agrees well (see Table 2).

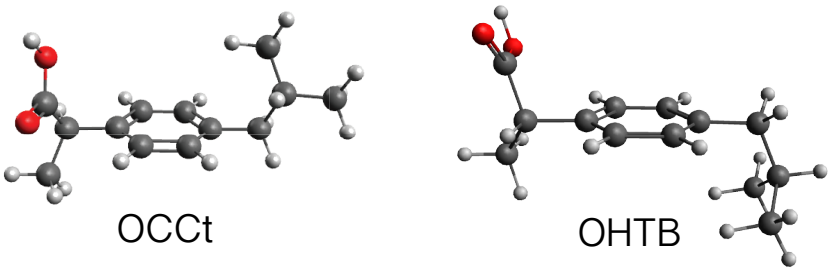

Figure 1: Labeling for two different conformers of ibuprofen.

A (MHz)	B (MHz)	C (MHz)	μ_A (D)	μ_B (D)	μ_C (D)	μ (D)	E (kJ/mol)	label
1330.50	261.29	251.80	-1.0689	-0.0409	1.1795	1.5923	0	O CCt (C1)
1354.98	262.89	249.51	-1.1333	-0.4097	1.3425	1.8041	0.15	O CCc (C2)
1576.42	246.96	240.81	1.1494	-0.7773	1.1749	1.8181	0.21	O TCc (C3)
1536.05	246.25	243.49	1.0361	0.2195	1.1643	1.5740	0.28	O TCt (C4)
1394.90	269.17	265.67	1.2051	-1.2353	0.3605	1.7630	1.81	O TB
1191.56	289.62	278.32	-1.2389	-0.4671	1.1602	1.7604	1.85	O CB
1331.17	258.77	251.14	-0.8285	-1.1525	-1.3544	1.9619	3.90	OHCCt
1347.50	260.58	249.94	-0.8430	-0.7056	-1.4432	1.8908	3.96	OHCCc
1606.47	243.88	238.82	-1.3042	1.5546	0.1805	2.0372	4.23	OHTCc
1577.83	242.51	240.79	-1.3030	-0.1272	-1.7303	2.1698	4.27	OHTCt
1180.11	287.56	279.49	-0.8869	-0.6566	-1.6149	1.9559	5.70	OHCB
1428.70	267.23	261.51	-1.4321	1.5191	0.4832	2.1429	5.88	OHTB

Table 1: Calculated molecular parameters for twelve low-lying conformers of ibuprofen using the M06-2X/6-31+G(d,p) level of theory. The label C1 to C4 indicates the four conformers assigned to the measured spectra.

A (MHz)	B (MHz)	C (MHz)	μ_A (D)	μ_B (D)	μ_C (D)	μ (D)	E (kJ/mol)	label
1320.01	253.15	244.88	-1.0295	-0.1045	1.2357	1.6177	0	O CCt
1351.94	253.54	242.19	-1.0922	-0.5065	1.3631	1.8186	0.09	O CCc
1538.75	238.39	236.29	1.0741	0.4258	1.1619	1.6369	0.12	O TCt
1573.22	239.21	233.88	1.1359	-0.7602	1.2388	1.8447	0.15	O TCc
1344.94	252.88	243.08	-0.9000	-0.7990	-1.4610	1.9828	3.79	OHCCc
1323.95	251.60	244.50	-0.9201	-1.2225	-1.3500	2.0404	3.82	OHCCt
1569.98	236.45	234.71	1.3826	-0.1650	1.7321	2.2224	3.87	OHTCt
1595.72	237.60	232.41	-1.3649	1.5760	0.1530	2.0905	3.95	OHTCc
1183.48	278.41	269.27	-1.7747	-0.5906	1.1843	1.7747	5.20	O CB
1401.17	260.07	255.90	1.2215	-1.2589	0.4316	1.8064	5.30	O TB
1177.98	277.43	270.28	-0.9691	-0.7572	-1.6400	8.9200	8.92	OHCB
1428.20	258.72	253.21	1.5121	1.5118	0.5065	2.1974	9.00	OHTB

Table 2: Calculated molecular parameters for twelve low-lying conformers of ibuprofen using the B3LYP/6-31+G(d,p) level of theory.

1.2 Internal Rotation

Internal rotation around a single bond can lead to line splittings of rotational transitions if the barrier for this rotation is low enough, i.e., if this is a feasible large-amplitude motion for the respective spectroscopic experiments. We do

parameter	C1	calc	C2	calc	C3	calc	C4	calc
A (MHz)	1325.656(3)	1337.0	1357.716(3)	1365.5	1570.534(4)	1585.4	1534.787(5)	1545.7
B (MHz)	260.7159(5)	263.3	261.4567(4)	264.3	245.4447(4)	248.6	244.8941(6)	247.7
C (MHz)	251.1813(5)	253.8	248.3119(4)	250.8	239.7532(5)	242.4	242.1034(6)	244.9
D_K (kHz)	0.89(21)		0.50(20)		0.69(48)		0.85(55)	
D_{JK} (kHz)	-0.049(14)		-0.068(12)		0.014(22)		0.013(22)	
D_J (kHz)	0.012(15)		0.012(13)		0.063(13)		0.067(15)	
μ_a (D)		-1.1		-1.2		1.2		1.1
μ_b (D)		-0.08		-0.5		-0.8		0.25
μ_c (D)		1.2		1.3		1.2		1.2
μ_{tot} (D)		1.7		1.9		1.9		1.7
E (kJ/mol)		0		0.13		0.12		0.19
assigned lines	139		151		113		109	
error (kHz)	33		31		29		38	

Table 3: Comparison of experimental and theoretical molecular parameters for the four lowest-energy conformers of ibuprofen including centrifugal distortion constants into the fit. The quantum-chemical calculations are performed at the DFT /M06-2X/aug-cc-pVTZ level of theory.

not observe this effect for ibuprofen. The calculated barrier heights for rotation around different single bonds (indicated in Figure 2) were calculated and the results for conformer 1 are listed in Table 4.

bond label	rotating group	barrier (kJ/mol)		
1	COOH	32.07	13.73	
2	CH_3	14.11	14.11	14.11
3	isopropyl	36.72	33.62	18.09
4	CH_3	15.95	15.95	15.95
5	CH_3	3.56	3.56	3.56

Table 4: Calculated barriers to internal rotation using the M06-2X/6-31+G(d,p) level of theory around five different single bonds in ibuprofen (see Figure 2). Different barriers for each group belong to several minimum positions during a full rotation of the group. All barriers were calculated for the lowest energy conformer C1.

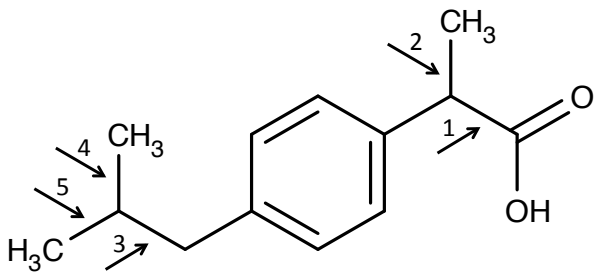

Figure 2: Labels for the calculated barriers to internal rotation around five different single bonds.

2 Potential fragments of Ibuprofen

In additional measurements where the sample was kept at the thermal decomposition temperature of ibuprofen for a longer time, two new spectra of previously uncharacterized species were observed. Each of the additional lines is split into two components. Both components of the doublets can be fitted individually with the fitted constants being summarized in Section 2.1 as two sets (F1 and F2). However, we cannot assign the respective molecular parameters to a specific molecular species.

However, it might be that the unknown spectra arise from ibuprofen fragments forming as a result of a decarboxylation process during heating [1, 2], and that the splitting arises from methyl-group internal rotation in such a fragment. Ab initio calculations were performed to shine more light onto this hypothesis. In Section 2.2, the theoretical results for two possible fragments are listed. These two fragments have, after decarboxylation, either an ethyl group or an ethyl radical attached to the phenyl ring (Figure 3). The results of calculations concerning the internal rotation in these fragments are listed in Section 2.3. In Section 2.4, we also present the results of geometry optimizations for fragment dimers to try to understand the origin of the spectrum denoted as F2.

2.1 Experimental Results

For both spectra, only a-type transitions described within the S-type reduced Watson-Hamiltonian in I^r reduction were observed and could be assigned to each component of the doublets individually. Interestingly, the rotational constants of the fragment F2 correspond almost exactly to half the values of the fragment F1. The results are listed in Table 5.

parameter	F1a	F1b	F2a	F2b
A (MHz)	2236.74	2220.11	1121.18	1118.78
B (MHz)	337.8	327.92	168.890	169.958
C (MHz)	320	320.02	159.885	160.005
assigned lines	20	20	34	45
mean error (kHz)	25	26	9	10

Table 5: Spectroscopic constants of the fragments. Here a and b correspond to the two components of the observed doublets..

2.2 Structure Calculations

In the following, the results of ab initio calculations regarding the two fragments of ibuprofen (Figure 3) are summarized. The results of these calculations are shown in Table 6 and 7, however, no decent agreement with the experimentally determined molecular parameters (Table 4) can be found.

2.3 Internal Rotation

The observed doublet lines could arise from internal rotation of a methyl group in the fragment. The fact that the two components of the doublets could be fitted individually indicates a high barrier case. The barrier for the internal

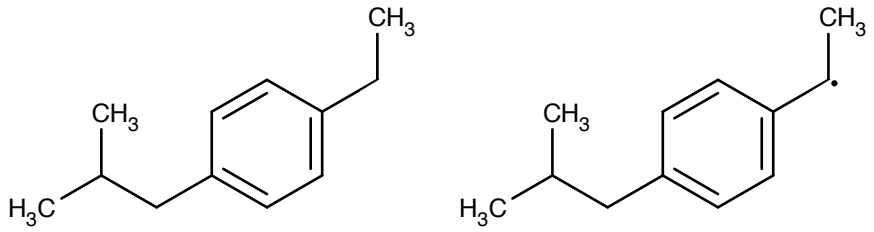

Figure 3: Two possible fragments of ibuprofen after COO- or COOH-release.

A (MHz)	B (MHz)	C (MHz)	μ_A (D)	μ_B (D)	μ_C (D)	μ (D)	E (kJ/mol)	label
2272.04	409.55	401.91	0.0971	0.0609	-0.2494	0.2745	0	CC
2776.53	393.02	379.97	-0.0978	-0.0956	0.1372	0.1938	0.02	TC
2278.77	446.75	420.42	-0.0096	-0.0122	-0.0531	0.0531	1.73	TB
1867.75	465.19	456.10	-0.0177	-0.0109	0.1641	0.1654	1.88	CB

Table 6: Calculated conformers of an ibuprofen fragment after CO_2 release using the M06-2X/6-31+G(d,p) level of theory.

A (GHz)	B (GHz)	C (GHz)	μ_A (D)	μ_B (D)	μ_C (D)	μ (D)	label	method	basis-set	energy (kJ/mol)
2554.86	404.50	387.36	-0.1809	-0.2547	-0.2094	0.3761	Ct	uM06-2X	6-31+G(d,p)	0
2615.16	405.19	383.85	0.1684	-0.0691	0.1789	0.2552	Cc	uM06-2X	6-31+G(d,p)	0.10
2104.45	462.51	429.31	0.0795	-0.1601	0.1247	0.2180	B	uM06-2X	6-31+G(d,p)	1.77
2634.91	394.03	374.10	0.0093	-0.0624	0.1109	0.1276	Cc	uB3LYP	6-31+G(d,p)	0
2550.95	394.39	377.15	-0.0158	-0.2698	0.1537	0.3109	Ct	uB3LYP	6-31+G(d,p)	0.05
2113.61	448.12	415.67	-0.0873	-0.1693	0.0493	0.1968	B	uB3LYP	6-31+G(d,p)	5.26
2649.25	397.80	376.94	0.0272	-0.0453	0.0887	0.1032	Cc	uB3LYP	cc-pvtz	0
2572.51	397.53	379.97	-0.0334	-0.2423	0.1250	0.2747	Ct	uB3LYP	cc-pvtz	0.06
2131.81	451.32	418.67	-0.0570	-0.1425	0.0095	0.1538	B	uB3LYP	cc-pvtz	5.27
2621.93	412.26	389.67	0.0544	-0.1251	0.1637	0.2131	Cc	uSVWN	6-31+G(d,p)	0
2561.33	410.85	392.70	-0.0682	-0.3439	0.2135	0.4105	Ct	uSVWN	6-31+G(d,p)	0.15
2106.56	473.32	439.11	-0.0266	-0.2310	0.1120	0.2581	B	uSVWN	6-31+G(d,p)	1.89
2609.08	407.55	387.35	0.0274	-0.0479	0.1159	0.1283	Cc	uMP2	aug-cc-pvdz	0
2540.60	407.26	389.90	-0.0399	-0.2170	0.1483	0.2659	Ct	uMP2	aug-cc-pvdz	0.20
2087.25	467.88	434.43	-0.0746	-0.1357	0.0501	0.1628	B	uMP2	aug-cc-pvdz	1.32

Table 7: Calculated conformers ofane ibuprofen fragment after COOH release using different theoretical methods.

rotation of the former α-methyl group (Figure 2, bond 2) of the two fragments, discussed in section 2.2, was calculated to identify for which fragment the barrier height could lead to the observed doublets. The results are listed in Table 8 and lead to the conclusion that the barriers are too high to expect a line splitting.

This conclusion is also supported by previous microwave studies of the related molecule ethylbenzene, which also does not show line splittings due to internal rotation of the terminal methyl top in the ethyl group under similar conditions [3].

fragment	rotating group	barrier (kJ/mol)
COOH-release	CH_3	5.74
CO_2-release	CH_3	15.03

Table 8: Barriers to internal rotation of the former α-methyl group using the M06-2X/6-31+G(d,p) level of theory.

2.4 Dimer Calculations

As the measured rotational constants of molecule F2 are approximately half the rotational constants of F1 (see section 2.2), calculations for fragment dimers were performed. The results are listed in Table 9 and the optimized structures are depicted in Figure 4. Again, no reasonable agreement with the experimental data could be found, so that the origin of the two characteristic rotational spectra F1 and F2 remain unknown for the moment.

Fragment dimer	A (MHz)	B (MHz)	C (MHz)	μ_A (D)	μ_B (D)	μ_C (D)	μ (D)	E (kJ/mol)
1	1058.67	63.38	63.25	0.0001	-0.0001	-0.0001	0.0014	0
2	251.61	153.51	105.91	-0.2673	-0.0463	-0.0083	0.2714	1.46
3	323.46	111.55	89.86	0.1037	0.045	0.1618	0.1973	2.59
4	414.39	102.19	96.59	-0.4641	-0.4641	0.2517	0.7012	78.19
5	311.19	186.84	132.40	-0.0094	0.0495	0.036	0.0619	355.87

Table 9: Calculated conformers of dimers of the discussed fragments using the M06-2X/6-31+G(d,p) level of theory. The different conformers arise from different orientations of the two fragments with respect to each other followed by structure optimization.

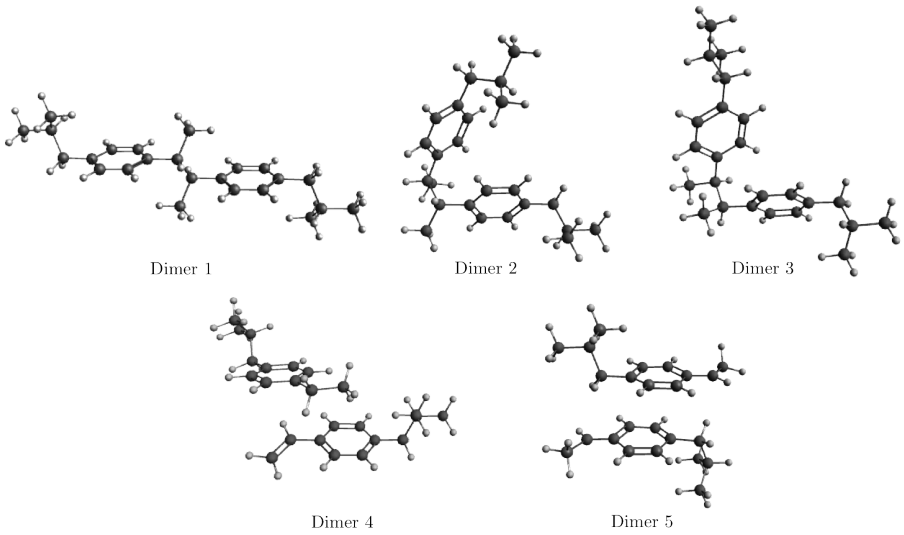

Figure 4: Optimized structure of five different dimers of the fragment. Calculations were performed using the M06-2X level of theory.

3 Line Lists of Observed Transitions

In the following table the assigned transitions for the four low-lying conformers of ibuprofen are listed. The quantum numbers describe a transition from $J'_{K'_a K'_c} \leftarrow J_{K_a K_c}$. The observed frequency and the strength of each transition are given in the table as well.

Conformer C1

J'	K'_a	K'_c	J	K_a	K_c	ν_{obs}(MHz)	ν_{obs}-ν_{calc}-**(kHz)**	strength (μV)
12	0	12	11	1	10	4706.6	4	48
9	0	9	8	1	7	3347.9	9	59
10	0	10	9	1	8	3808.4	31	58
11	0	11	10	0	10	5617	-4	200
12	0	12	11	0	11	6124.9	3	180
13	0	13	12	0	12	6632.1	20	150
14	0	14	13	0	13	7138.6	23	130
4	0	4	3	0	3	2046.9	-49	94
5	0	5	4	0	4	2558.2	-6	130
6	0	6	5	0	5	3069.1	2	160
7	0	7	6	0	6	3579.7	-4	190
8	0	8	7	0	7	4089.8	-23	210
9	0	9	8	0	8	4599.4	-47	210
10	0	10	9	0	9	5108.5	0	210
11	1	11	10	1	10	5575.1	-23	70
12	1	11	11	1	10	6195.2	14	160
12	1	12	11	1	11	6081.3	14	170
13	1	12	12	1	11	6710.4	-1	140
13	1	13	12	1	12	6587.3	9	140
14	1	13	13	1	12	7225.4	-35	120
14	1	14	13	1	13	7093.1	-15	120
15	1	14	14	1	13	7740.2	44	95
15	1	15	14	1	14	7598.8	-2	98
4	1	3	3	1	2	2066.5	-28	84
4	1	4	3	1	3	2028.4	11	83
5	1	5	4	1	4	2535.4	33	120
6	1	6	5	1	5	3042.3	33	150
7	1	6	6	1	5	3615.8	17	180
7	1	7	6	1	6	3549.1	26	180
8	1	7	7	1	6	4132	16	200
8	1	8	7	1	7	4055.8	25	190
9	1	8	8	1	7	4648.1	6	200
9	1	9	8	1	8	4562.4	19	200
10	1	9	9	1	8	5163.9	1	200
10	1	10	9	1	9	5068.8	-11	200
11	1	10	10	1	9	5679.6	-53	180
12	2	11	11	2	10	6139.8	-21	140
13	2	11	12	2	10	6673.4	14	120
13	2	12	12	2	11	6650.9	17	120
14	2	13	13	2	12	7161.8	-5	100
15	2	13	14	2	12	7706.4	-32	81
5	2	4	4	2	3	2559.3	-40	90
6	2	5	5	2	4	3071.1	12	120
7	2	5	6	2	4	3586.3	-32	140

J'	K'_a	K'_c	J	K_a	K_c	ν_{obs}(MHz)	ν_{obs}-ν_{calc}-**(kHz)**	strength (μV)
7	2	6	6	2	5	3582.8	29	140
8	2	6	7	2	5	4099.7	-9	160
8	2	7	7	2	6	4094.4	23	160
9	2	7	8	2	6	4613.5	8	170
9	2	8	8	2	7	4605.9	4	170
10	2	8	9	2	7	5127.7	-23	160
10	2	9	9	2	8	5117.4	34	160
11	2	9	10	2	8	5642.4	-32	150
11	2	10	10	2	9	5628.6	-74	150
11	2	10	10	2	9	5628.6	-74	150
12	2	10	11	2	9	6157.6	-28	140
13	3	11	12	3	10	6657.2	-9	91
14	3	12	13	3	11	7169.7	-8	76
15	3	12	14	3	11	7683.8	8	61
15	3	13	14	3	12	7682.2	16	61
6	3	3	5	3	2	3071.7	-37	78
6	3	4	5	3	3	3071.7	-22	78
7	3	4	6	3	3	3583.8	-18	99
7	3	5	6	3	4	3583.8	16	99
8	3	5	7	3	4	4096	2	110
8	3	6	7	3	5	4096	70	110
9	3	6	8	3	5	4608.2	18	120
10	3	7	9	3	6	5120.4	-75	120
10	3	8	9	3	7	5120.3	36	120
11	3	8	10	3	7	5632.9	25	110
11	3	9	10	3	8	5632.5	-32	110
13	3	10	12	3	9	6658	-23	91
15	4	11	14	4	10	7680.9	11	42
7	4	3	6	4	2	3583.6	7	57
7	4	4	6	4	3	3583.6	7	57
8	4	4	7	4	3	4095.6	-14	69
8	4	5	7	4	4	4095.6	-14	69
9	4	5	8	4	4	4607.7	32	76
9	4	6	8	4	5	4607.7	33	76
10	4	6	9	4	5	5119.8	11	77
10	4	7	9	4	6	5119.8	13	77
11	4	7	10	4	6	5631.9	14	75
11	4	8	10	4	7	5631.9	17	75
12	4	8	11	4	7	6144.1	41	69
12	4	9	11	4	8	6144.1	47	69
13	4	9	12	4	8	6656.3	9	60
13	4	10	12	4	9	6656.3	19	60
9	5	4	8	5	3	4607.6	72	41
9	5	5	8	5	4	4607.6	72	41
10	5	5	9	5	4	5119.5	1	43
10	5	6	9	5	5	5119.5	1	43
11	5	6	10	5	5	5631.5	-47	43
11	5	7	10	5	6	5631.5	-47	43
12	5	7	11	5	6	6143.6	-8	40
12	5	8	11	5	7	6143.6	-8	40
13	5	8	12	5	7	6655.7	-4	36
13	5	9	12	5	8	6655.7	-4	36
12	6	6	11	6	5	6143.4	-18	21

J'	K'_a	K'_c	J	K_a	K_c	ν_{obs}(MHz)	ν_{obs}-ν_{calc}-**(kHz)**	strength (μV)
12	6	7	11	6	6	6143.4	-18	21
4	2	3	4	1	3	3161.6	19	62
5	2	4	5	1	4	3137.8	-60	69
5	2	3	5	1	5	3283.1	-7	68
7	2	5	7	1	7	3351.4	-16	68
9	2	7	9	1	9	3446.5	16	55
12	3	10	12	2	10	5303.3	28	45
13	3	11	13	2	11	5287.1	5	36
13	3	10	13	2	12	5374.7	-45	36
6	3	4	6	2	4	5345.4	119	88
7	3	5	7	2	5	5342.7	16	89
7	3	4	7	2	6	5350.8	39	89
8	3	6	8	2	6	5338.9	32	84
8	3	5	8	2	7	5352.4	53	85
10	3	8	10	2	8	5326	2	67
11	3	9	11	2	9	5315.9	-167	56
13	4	10	13	3	10	7481.6	24	36
14	4	11	14	3	11	7479.3	7	28
5	4	1	5	3	3	7487.6	-51	63
12	1	11	11	0	11	7613.4	24	100
3	1	2	2	0	2	2634	-26	64
4	1	3	3	0	3	3165.1	-19	88
5	1	4	4	0	4	3701.2	-7	110
7	1	6	6	0	6	4789.1	1	140
8	1	7	7	0	7	5341.3	-39	140
9	1	8	8	0	8	5899.6	1	140
10	1	9	9	0	9	6464.1	7	130
2	2	1	1	1	1	4237.7	38	74
3	2	1	2	1	1	4730.8	-16	88
3	2	2	2	1	2	4759.1	-3	87
4	2	2	3	1	2	5229	-14	100
4	2	3	3	1	3	5285.3	8	100
4	2	3	3	1	3	5285.3	8	100
6	2	4	5	1	4	6213.4	-5	120
6	2	5	5	1	5	6352	2	120
7	2	5	6	1	5	6700.3	-9	130
7	2	6	6	1	6	6892.5	32	120
8	2	6	7	1	6	7184.2	-2	120
9	2	7	8	1	7	7665.7	-10	120
3	3	0	2	2	0	6884.1	-1	150
3	3	1	2	2	1	6884.3	42	150
3	3	1	2	2	1	6884.1	-64	150

Table 10: Observed Transitions of Conformer C1

Conformer C2

J'	K'_a	K'_c	J	K_a	K_c	ν_{obs}(MHz)	ν_{obs}-ν_{calc}-**(kHz)**	strength (μV)
12	0	12	11	1	10	4486.6	10	85
13	0	13	12	1	11	4885.8	15	71
14	0	14	13	1	12	5271.7	-21	56
14	0	14	13	1	12	5271.7	-15	56
15	0	15	14	1	13	5643.9	-6	43
12	0	12	11	0	11	6084.8	-15	350

J'	K'_a	K'_c	J	K_a	K_c	ν_{obs}(MHz)	ν_{obs}-ν_{calc}-**(kHz)**	strength (μV)
13	0	13	12	0	12	6586.3	-20	310
14	0	14	13	0	13	7086.8	3	260
15	0	15	14	0	14	7586.2	-3	210
4	0	4	3	0	3	2037.9	3	190
5	0	5	4	0	4	2546.5	10	260
6	0	6	5	0	5	3054.5	1	330
7	0	7	6	0	6	3561.8	-14	380
8	0	8	7	0	7	4068.4	29	420
9	0	9	8	0	8	4574	12	430
10	0	10	9	0	9	5078.6	-18	420
11	1	11	10	1	10	5529.2	-11	140
11	1	11	10	1	10	5529.2	-11	140
12	1	11	11	1	10	6187.1	-15	330
12	1	12	11	1	11	6030.7	7	340
13	1	12	12	1	11	6700.8	-21	290
13	1	13	12	1	12	6531.9	37	290
14	1	13	13	1	12	7214	-18	240
15	1	14	14	1	13	7726.6	-25	190
15	1	15	14	1	14	7533.5	-6	200
4	1	3	3	1	2	2065.1	-27	170
5	1	4	4	1	3	2581.2	19	240
5	1	5	4	1	4	2515.3	-147	240
6	1	5	5	1	4	3097.1	20	310
6	1	6	5	1	5	3018.2	-25	300
7	1	6	6	1	5	3612.8	10	360
7	1	7	6	1	6	3520.9	28	360
8	1	7	7	1	6	4128.3	27	390
8	1	8	7	1	7	4023.3	23	390
9	1	8	8	1	7	4643.5	0	400
9	1	9	8	1	8	4525.5	11	400
10	1	9	9	1	8	5158.4	0	390
10	1	10	9	1	9	5027.5	28	400
11	1	10	10	1	9	5673	12	370
4	2	2	3	2	1	2040	-157	110
12	2	11	11	2	10	6111.9	6	280
13	2	11	12	2	10	6660.7	36	240
14	2	12	13	2	11	7177.9	-9	200
14	2	13	13	2	12	7128.1	-22	200
15	2	13	14	2	12	7695.9	-15	160
15	2	14	14	2	13	7635.9	24	160
5	2	3	4	2	2	2551	37	180
5	2	4	4	2	3	2548.6	21	180
6	2	4	5	2	3	3062.2	21	240
6	2	5	5	2	4	3058.1	12	240
7	2	5	6	2	4	3574	-4	290
7	2	6	6	2	5	3567.5	31	290
8	2	6	7	2	5	4086.5	15	320
8	2	7	7	2	6	4076.7	6	320
9	2	7	8	2	6	4599.7	5	330
9	2	8	8	2	7	4585.8	26	330
10	2	8	9	2	7	5113.7	8	330
10	2	9	9	2	8	5094.7	23	330
11	2	9	10	2	8	5628.6	41	310

J'	K'_a	K'_c	J	K_a	K_c	ν_{obs}(MHz)	ν_{obs}-ν_{calc}-**(kHz)**	strength (μV)
11	2	10	10	2	9	5603.4	18	310
11	2	10	10	2	9	5603.4	18	310
12	2	10	11	2	9	6144.1	-29	280
13	3	11	12	3	10	6631.6	16	180
14	3	11	13	3	10	7145.1	2	150
14	3	12	13	3	11	7142.3	12	150
15	3	12	14	3	11	7657	-4	120
7	3	4	6	3	3	3569.3	-91	200
7	3	5	6	3	4	3569.3	-1	200
9	3	6	8	3	5	4590	-9	240
9	3	7	8	3	6	4589.7	-6	240
10	3	7	9	3	6	5100.6	41	240
10	3	8	9	3	7	5100	-40	240
11	3	9	10	3	8	5610.5	-11	230
12	3	9	11	3	8	6122.3	11	210
12	3	10	11	3	9	6121	17	210
13	3	10	12	3	9	6633.5	-30	180
14	4	11	13	4	10	7140.6	84	100
7	4	3	6	4	2	3569	35	110
7	4	4	6	4	3	3569	36	110
9	4	5	8	4	4	4589	-32	150
9	4	6	8	4	5	4589	-30	150
10	4	6	9	4	5	5099.2	10	150
10	4	7	9	4	6	5099.2	16	150
11	4	7	10	4	6	5609.4	11	150
11	4	8	10	4	7	5609.4	21	150
12	4	8	11	4	7	6119.7	-12	140
12	4	9	11	4	8	6119.7	7	140
14	4	10	13	4	9	7140.6	25	100
9	5	4	8	5	3	4588.7	15	79
9	5	5	8	5	4	4588.7	15	79
10	5	5	9	5	4	5098.7	15	84
10	5	6	9	5	5	5098.7	15	84
12	5	7	11	5	6	6118.7	-83	78
12	5	8	11	5	7	6118.7	-83	78
14	5	9	13	5	8	7139.2	7	60
14	5	10	13	5	9	7139.2	7	60
9	6	3	8	6	2	4588.5	-12	36
9	6	4	8	6	3	4588.5	-12	36
10	6	4	9	6	3	5098.5	13	40
10	6	5	9	6	4	5098.5	13	40
12	2	11	12	1	11	2808.2	-14	70
3	2	1	3	1	3	3348.6	12	100
4	2	2	4	1	4	3376.2	3	130
5	2	3	5	1	5	3411.7	43	140
6	2	5	6	1	5	3171.4	26	150
6	2	4	6	1	6	3455.6	8	140
7	2	5	7	1	7	3508.8	11	140
8	2	6	8	1	8	3571.9	-16	130
10	2	9	10	1	9	2953	-20	100
11	3	8	11	2	10	5539.3	-32	54
12	3	10	12	2	10	5431.5	-7	51
12	3	9	12	2	11	5549.8	29	51

J'	K'_a	K'_c	J	K_a	K_c	ν_{obs}(MHz)	ν_{obs}-ν_{calc}-**(kHz)**	strength (μV)
16	3	14	16	2	14	5273.2	14	29
4	3	2	4	2	2	5512.7	-36	32
5	3	3	5	2	3	5511.1	17	42
5	3	2	5	2	4	5515.2	-11	42
6	3	4	6	2	4	5508.2	14	49
6	3	3	6	2	5	5516.4	2	49
7	3	5	7	2	5	5503.5	51	54
7	3	4	7	2	6	5518.4	54	54
8	3	6	8	2	6	5496.4	-24	56
8	3	5	8	2	7	5521.3	24	57
9	3	7	9	2	7	5486.4	-34	57
9	3	6	9	2	8	5525.5	-15	57
9	3	6	9	2	8	5525.5	-15	57
11	3	9	11	2	9	5454.7	-26	54
5	4	2	5	3	2	7719.4	16	130
5	4	1	5	3	3	7719.4	-2	130
2	1	1	1	0	1	2142.1	13	84
11	1	10	10	0	10	7180.5	26	230
12	1	11	11	0	11	7785.3	-41	200
3	1	2	2	0	2	2671.6	-18	130
5	1	4	4	0	4	3751.2	6	220
8	1	7	7	0	7	5426.5	-34	76
9	1	8	8	0	8	6001.7	7	280
10	1	9	9	0	9	6586.1	-34	260
2	2	1	1	1	1	4334.6	2	150
3	2	2	2	1	2	4857.5	-13	180
4	2	3	3	1	2	5308.1	-8	32
4	2	2	3	1	2	5309.9	30	210
5	2	3	4	1	4	5927.1	-24	34
5	2	4	4	1	4	5923	-14	230
6	2	4	5	1	4	6276.7	33	250
6	2	5	5	1	5	6465.6	-24	240
7	2	5	6	1	5	6753.6	9	260
7	2	6	6	1	6	7014.8	-2	240
8	2	6	7	1	6	7227.3	14	260
8	2	7	7	1	7	7570.7	28	240
9	2	7	8	1	7	7698.7	-9	250
3	3	0	2	2	0	7043.4	7	320
3	3	1	2	2	1	7043.4	-67	320

Table 11: Observed Transitions of Conformer C2

Conformer C3

J'	K'_a	K'_c	J	K_a	K_c	ν_{obs}(MHz)	ν_{obs}-ν_{calc}-**(kHz)**	strength (μV)
14	0	14	13	1	12	5178.9	2	83
11	0	11	10	0	10	5333.1	-5	410
13	0	13	12	0	12	6300.9	-8	330
14	0	14	13	0	13	6784.4	-60	280
15	0	15	14	0	14	7267.8	28	230
5	0	5	4	0	4	2425.6	-21	260
6	0	6	5	0	5	2910.6	58	330
7	0	7	6	0	6	3395.4	6	390
8	0	8	7	0	7	3880	-35	420

J'	K'_a	K'_c	J	K_a	K_c	ν_{obs}(MHz)	ν_{obs}-ν_{calc}-**(kHz)**	strength (μV)
9	0	9	8	0	8	4364.6	29	440
10	0	10	9	0	9	4849	13	440
11	1	11	10	1	10	5304.9	13	390
11	1	11	10	1	10	5304.9	13	390
12	1	11	11	1	10	5855.2	44	350
12	1	12	11	1	11	5786.9	-8	350
13	1	12	12	1	11	6342.8	-12	310
13	1	13	12	1	12	6268.9	-15	310
14	1	13	13	1	12	6830.4	0	260
14	1	14	13	1	13	6750.9	-5	260
15	1	14	14	1	13	7317.8	-85	210
15	1	15	14	1	14	7232.8	0	220
6	1	5	5	1	4	2928.1	-10	300
6	1	6	5	1	5	2894	-10	300
7	1	6	6	1	5	3416.1	28	360
7	1	7	6	1	6	3376.2	-18	350
8	1	8	7	1	7	3858.4	-9	390
9	1	8	8	1	7	4391.8	-1	410
9	1	9	8	1	8	4340.6	-32	410
10	1	9	9	1	8	4879.7	38	400
10	1	10	9	1	9	4822.8	18	410
11	1	10	10	1	9	5367.4	11	380
12	2	11	11	2	10	5821.5	-6	280
13	2	11	12	2	10	6313.1	29	250
13	2	12	12	2	11	6306.5	20	250
14	2	13	13	2	12	6791.4	-2	210
16	2	15	15	2	14	7761.1	47	140
5	2	3	4	2	2	2426.3	-43	170
6	2	4	5	2	3	2911.7	-40	230
7	2	5	6	2	4	3397.3	-2	280
7	2	6	6	2	5	3396.2	4	280
8	2	6	7	2	5	3882.9	18	310
8	2	7	7	2	6	3881.3	-46	310
9	2	7	8	2	6	4368.6	-25	320
9	2	8	8	2	7	4366.4	-33	320
10	2	8	9	2	7	4854.5	-3	320
10	2	9	9	2	8	4851.5	10	320
11	2	9	10	2	8	5340.5	-27	310
11	2	10	10	2	9	5336.5	-16	310
14	3	11	13	3	10	6793.9	31	150
14	3	12	13	3	11	6793.7	0	150
15	3	12	14	3	11	7279.3	-8	120
15	3	13	14	3	12	7279.1	-1	120
8	3	5	7	3	4	3881.8	6	210
8	3	6	7	3	5	3881.8	16	210
9	3	6	8	3	5	4367.1	13	220
9	3	7	8	3	6	4367.1	30	220
10	3	7	9	3	6	4852.4	21	220
10	3	8	9	3	7	4852.4	50	220
11	3	8	10	3	7	5337.7	-7	220
11	3	9	10	3	8	5337.7	41	220
14	4	11	13	4	10	6793.3	2	93
15	4	11	14	4	10	7278.6	-13	77

J'	K'_a	K'_c	J	K_a	K_c	ν_{obs}(MHz)	ν_{obs}-ν_{calc}-**(kHz)**	strength (μV)
15	4	12	14	4	11	7278.6	-11	77
10	4	6	9	4	5	4852.2	30	130
10	4	7	9	4	6	4852.2	30	130
11	4	7	10	4	6	5337.4	-45	130
11	4	8	10	4	7	5337.4	-45	130
12	4	8	11	4	7	5822.7	-18	120
12	4	9	11	4	8	5822.7	-17	120
14	4	10	13	4	9	6793.3	0	93
11	2	10	11	1	10	3797.3	71	120
3	2	2	3	1	2	3966.8	45	120
3	2	1	3	1	3	4001	-24	120
4	2	3	4	1	3	3955.4	13	160
4	2	2	4	1	4	4012.6	2	160
5	2	3	5	1	5	4027.2	-1	170
6	2	5	6	1	5	3924.2	33	180
6	2	4	6	1	6	4045	21	180
7	2	5	7	1	7	4066	-20	180
8	2	6	8	1	8	4090.5	16	170
9	2	8	9	1	8	3856.3	-22	160
9	2	7	9	1	9	4118.4	-55	150
11	3	8	11	2	10	6643.4	-10	150
12	3	9	12	2	11	6645	-2	120
13	3	11	13	2	11	6621.8	-44	97
13	3	10	13	2	12	6647	12	97
14	3	12	14	2	12	6615.9	-10	76
14	3	11	14	2	13	6649.5	8	76
9	3	6	9	2	8	6641.4	37	190
10	3	7	10	2	9	6642.2	-27	170
11	3	9	11	2	9	6630.3	42	150
11	1	10	10	0	10	6858.8	38	270
11	1	10	10	0	10	6858.8	38	270
3	1	2	2	0	2	2800.6	-13	140
4	1	3	3	0	3	3297.2	-30	190
5	1	4	4	0	4	3796.8	-5	240
7	1	6	6	0	6	4804.8	-4	300
8	1	7	7	0	7	5313.4	-1	310
8	1	7	7	0	7	5313.4	-4	310
9	1	8	8	0	8	5825.2	23	310
10	1	9	9	0	9	6340.3	27	290
3	2	1	2	1	1	5430.9	-42	41
3	2	2	2	1	2	5448	36	41
4	2	2	3	1	2	5907.8	7	230
4	2	3	3	1	3	5941.7	-3	230
5	2	3	4	1	3	6381.9	-25	250
5	2	3	4	1	3	6381.9	-25	250
5	2	4	4	1	4	6438.2	-37	250
6	2	4	5	1	4	6853.5	-59	270
6	2	5	5	1	5	6937.7	41	260
7	2	5	6	1	5	7322.8	55	270
7	2	6	6	1	6	7439.9	-17	270
8	2	7	7	1	7	7945	-42	260

Table 12: Observed Transitions of Conformer C3

Conformer C4

J'	K'_a	K'_c	J	K_a	K_c	ν_{obs}(MHz)	ν_{obs}-ν_{calc}-**(kHz)**	strength (μV)
10	0	10	9	1	8	3514	24	130
11	0	11	10	0	10	5355.9	-40	410
12	0	12	11	0	11	5842.6	-28	370
14	0	14	13	0	13	6815.8	-34	280
15	0	15	14	0	14	7302.4	28	230
16	0	16	15	0	15	7788.8	15	180
5	0	5	4	0	4	2434.9	7	260
6	0	6	5	0	5	2921.8	-20	330
7	0	7	6	0	6	3408.7	-19	380
8	0	8	7	0	7	3895.6	15	420
9	0	9	8	0	8	4382.4	-14	440
10	0	10	9	0	9	4869.2	0	430
11	1	11	10	1	10	5341.3	-4	380
12	1	11	11	1	10	5860.3	-35	350
13	1	12	12	1	11	6348.6	-16	300
14	1	14	13	1	13	6797.8	-11	260
15	1	14	14	1	13	7325.2	9	210
15	1	15	14	1	14	7283.4	34	210
5	1	4	4	1	3	2441.9	-41	230
5	1	5	4	1	4	2428	25	230
6	1	6	5	1	5	2913.6	0	300
7	1	6	6	1	5	3418.7	19	350
7	1	7	6	1	6	3399.1	-45	350
8	1	7	7	1	6	3907	-38	390
8	1	8	7	1	7	3884.7	-11	390
9	1	8	8	1	7	4395.4	16	410
10	1	9	9	1	8	4883.7	-19	400
10	1	10	9	1	9	4855.8	-12	400
11	1	10	10	1	9	5372	-30	380
12	2	11	11	2	10	5843.7	-24	280
14	2	12	13	2	11	6819.6	-2	210
15	2	14	14	2	13	7304.5	-11	170
16	2	14	15	2	13	7794.4	-23	140
16	2	15	15	2	14	7791.4	51	140
6	2	5	5	2	4	2922	54	230
7	2	5	6	2	4	3409.2	11	280
8	2	6	7	2	5	3896.3	12	310
9	2	8	8	2	7	4382.9	22	320
10	2	8	9	2	7	4870.6	26	320
10	2	9	9	2	8	4869.8	-36	320
11	2	9	10	2	8	5357.8	59	310
11	2	10	10	2	9	5356.8	15	310
12	2	10	11	2	9	5845	-3	280
14	3	11	13	3	10	6818.1	-79	150
14	3	12	13	3	11	6818.1	-60	150
15	3	12	14	3	11	7305.2	-11	120
15	3	13	14	3	12	7305.2	16	120
16	3	13	15	3	12	7792.1	-128	99
16	3	14	15	3	13	7792.1	-90	99
7	3	4	6	3	3	3409	-10	180
7	3	5	6	3	4	3409	-10	180

J'	K'_a	K'_c	J	K_a	K_c	ν_{obs}(MHz)	ν_{obs}-ν_{calc}-**(kHz)**	strength (μV)
8	3	5	7	3	4	3896	-20	210
8	3	6	7	3	5	3896	-19	210
11	3	8	10	3	7	5357.1	28	220
11	3	9	10	3	8	5357.1	34	220
12	3	9	11	3	8	5844.1	2	200
12	3	10	11	3	9	5844.1	11	200
14	4	11	13	4	10	6818.1	51	94
15	4	11	14	4	10	7305.1	22	78
15	4	12	14	4	11	7305.1	22	78
16	4	12	15	4	11	7792.1	71	62
16	4	13	15	4	12	7792.1	71	62
10	4	6	9	4	5	4870.1	95	130
10	4	7	9	4	6	4870.1	95	130
14	4	10	13	4	9	6818.1	51	94
10	2	8	10	1	10	3953.1	37	130
12	2	10	12	1	12	3987.6	3	91
14	2	12	14	1	14	4029.3	18	56
4	2	2	4	1	4	3887.9	22	150
5	2	3	5	1	5	3895	45	170
7	2	6	7	1	6	3834.9	26	180
7	2	5	7	1	7	3913.6	23	180
8	2	7	8	1	7	3823.7	-13	170
8	2	6	8	1	8	3925.1	-2	170
9	2	8	9	1	8	3811.2	-6	150
10	2	9	10	1	9	3797.3	-24	130
12	3	10	12	2	10	6453.2	33	120
13	3	11	13	2	11	6452	-4	95
14	3	12	14	2	12	6450.5	-23	74
14	3	11	14	2	13	6458.7	-14	74
15	3	13	15	2	13	6448.7	-62	56
15	3	12	15	2	14	6459.5	30	56
16	3	13	16	2	15	6460.3	-77	41
10	3	8	10	2	8	6454.8	15	170
11	3	9	11	2	9	6454.1	19	140
11	1	10	10	0	10	6741.8	14	270
12	1	11	11	0	11	7246.2	-24	240
13	1	12	12	0	12	7752.2	3	200
3	1	2	2	0	2	2760.7	11	140
5	1	4	4	0	4	3747.2	-38	230
6	1	5	5	0	5	4242.7	40	270
7	1	6	6	0	6	4739.5	-20	290
8	1	7	7	0	7	5237.8	-39	310
9	1	8	8	0	8	5737.6	-13	300
10	1	9	9	0	9	6238.9	-24	290
3	2	1	2	1	1	5330.7	-13	200
3	2	2	2	1	2	5338.9	-88	200
4	2	2	3	1	2	5813.6	32	220
4	2	3	3	1	3	5830.2	-8	220
5	2	3	4	1	3	6295	-12	240
5	2	4	4	1	4	6322.8	17	240
6	2	4	5	1	4	6775.2	-9	260
6	2	5	5	1	5	6816.8	3	260
7	2	5	6	1	5	7254.1	17	260

J'	K'_a	K'_c	J	K_a	K_c	ν_{obs}(MHz)	ν_{obs}-ν_{calc}-**(kHz)**	strength (μV)
7	2	6	6	1	6	7312.1	-26	260
8	2	6	7	1	6	7731.7	10	260
8	2	7	7	1	7	7808.9	7	250
3	3	0	2	2	0	7917.4	38	340
3	3	1	2	2	1	7917.4	34	340

Table 13: Observed Transitions of Conformer C4

References

[1] M. A. Zayed, M. F. Hawash, M. A. Fahmey, A. M. M. El-Gizouli, *Journal of Thermal Analysis and Calorimetry* **2012**, *108*(1), 315–322.

[2] G. Caviglioli, P. Valeria, P. Brunella, C. Sergio, A. Attilia, B. Gaetano, *Journal of Pharmaceutical and Biomedical Analysis* **2002**, *30*(3), 499 – 509.

[3] W. Caminati, D. Damiani, G. Corbelli, B. Velino, C. W. Bock, *Molecular Physics* **1991**, *74*(4), 885–895.